When CVaR Meets With Bluetooth PAN: A Physical Distancing System for COVID-19 Proactive Safety

Md. Shirajum Munir, *Graduate Student Member, IEEE*, Do Hyeon Kim, Anupam Kumar Bairagi, *Member, IEEE*, and Choong Seon Hong, *Senior Member, IEEE*

***Abstract*—In this work, we propose a risk-aware physical distancing system to assure a private safety distance from others for reducing the chance of being affected by the COVID-19 or such kind of pandemic. In particular, we have formulated a physical distancing problem by capturing Conditional Value-at-Risk (CVaR) of a Bluetooth-enabled personal area network (PAN). To solve the formulated risk-aware physical distancing problem, we propose two stages solution approach by imposing control flow, linear model, and curve-fitting schemes. Notably, in the first stage, we determine a PAN creator's safe movement distance by proposing a probabilistic linear model. This scheme can effectively cope with a tail-risk from the probability distribution by satisfying the CVaR constraint for estimating safe movement distance. In the second stage, we design a Levenberg-Marquardt (LM)-based curve fitting algorithm upon the recommended safety distance and current distances between the PAN creator and others to find an optimal high-risk trajectory plan for the PAN creator. Finally, we have performed an extensive performance analysis using state-of-the-art Bluetooth data to establish the proposed risk-aware physical distancing system's effectiveness. Our experimental results show that the proposed solution approach can effectively reduce the risk of recommending safety distance towards ensuring private safety. In particular, for a 95% CVaR confidence, we can successfully deal with 45.11% of the risk for measuring the PAN creator's safe movement distance.**

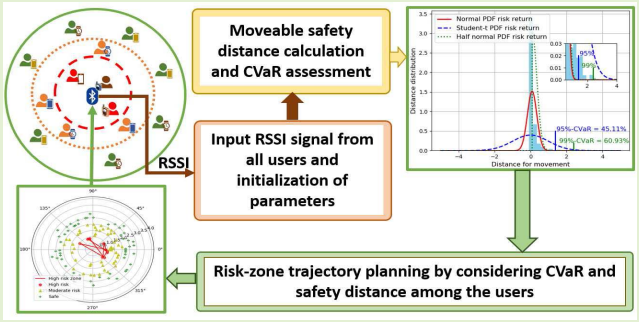

***Index Terms*— Physical distancing, conditional value-at-risk (CVaR), personal area network (PAN), Bluetooth, COVID-19.**

I. Introduction

A. Background and Motivation

NOWADAYS, the outbreak of Coronavirus disease 2019 (COVID-19) is a global crisis that can prevent by keeping a certain physical distance among individuals [1]. It is imperative to take necessary preventive measures to *flatten the curve* of COVID-19. In particular, increasing the physical space among the individuals can help to maintain the social distance and smooth the trajectory of COVID-19 affected cases. Maintaining a certain physical distance by the individuals can establish a social connection to promote resilient communities for adapting to the changes in society. This also can reduce the stresses and metal fatigue [2], and other disturbances due to pandemic. Hence, to assure physical distancing, recommending a safe distance from others is possible by utilizing communication technologies. In particular, by using existing smart devices (e.g., smart-phone, smart-watch, smart wearable), a distance can be measured among the individuals and recommend the safe space and a risk-zone trajectory by analyzing personal safety risk.

Significantly, the Internet of Things (IoT) technologies [3]–[7] are promising to show such distance measurement and other services for the smart city [8] and its citizens by establishing IoT networks [9], [10], and wireless networks [11] infrastructure. Besides, a personal area network (PAN) can create by utilizing Bluetooth technologies [3]–[7] to measure the physical distance between two IoT devices of both

Manuscript received February 22, 2021; accepted March 19, 2021. Date of publication March 24, 2021; date of current version June 14, 2021. This work was supported in part by the Institute of Information and Communications Technology Planning and Evaluation (IITP) Grant by the Korean Government through MSIT (Evolvable deep learning model generation platform for edge computing) under Grant 2019-0-01287 and in part by the MSIT Korea through the Grand Information Technology Research Center Support Program supervised by the Institute of Information and Communications Technology Planning and Evaluation (IITP) under Grant IITP-2020-2015-0-00742. This article was presented at the Proceedings of Korea Computer Congress 2020. The associate editor coordinating the review of this article and approving it for publication was Prof. Subhas C. Mukhopadhyay. *(Corresponding author: Choong Seon Hong.)*

The authors are with the Department of Computer Science and Engineering, Kyung Hee University, Yongin 17104, Republic of Korea (e-mail: munir@khu.ac.kr; doma@khu.ac.kr; anupam@khu.ac.kr; cshong@khu.ac.kr).

Digital Object Identifier 10.1109/JSEN.2021.3068782

indoor and outdoor environments. Further, the significance of using Bluetooth beacon for measuring physical distance is the capability of less interference between Bluetooth and other wireless technologies, since a frequency hopping spread spectrum (FHSS) technique is used. In particular, it utilizes a spectrum range between 2.402 and 2.480 GHz, or 2.400 and 2.4835 GHz with a 2 MHz wide guard band [12]. Thus, a Bluetooth-based PAN in a close-proximity environment can efficiently measure a distance between two IoT devices through a received signal strength indicator (RSSI).

Recently, Apple and Google have exposed the *Contact Tracing* APIs for Bluetooth to track and inform the users' contact with others, in which Rolling Proximity Identifiers are changed every 15 minutes on average. Thus, this approach is a post-measurement and does not in a real-time manner [7], [13]. On the other hand, Bluetooth could get its wrong distance when the signal passes through the environmental obstacle such as the human body and physical substance [6]. Thus, considering environmental factors [3] is an effective way to reduce the error of distance measurement through the RSSI. In which, applying additional risk measurement can deal to reduce that error. In particular, Conditional Value-at-Risk (CVaR) [9], [10], [14] is a risk assessment metric that has the potential for coping with a tail-risk of measuring a reliable safety distance in PAN by capturing uncertainty. In this work, we focus on address the following research questions:

1) Can Bluetooth measure the distance with reliability?
2) Can we take a proactive private safety distance measure?
3) How to ensure the right decision within 200 to 1000 ms for recommending a safety distance in PAN?

In the context of a risk-aware physical distancing system for COVID-19 or such kind of pandemic, this work provides a reliable and proactive physical distancing solution for society. In particular, we assume that the proposed physical distancing system's users are not already affected or diagnosed by the COVID-19. The objective of this work is to encourage and maintain social distancing [15], [16] among the general people of the society for assuring private safety and better mental health [2]. However, in general, the asymptomatic COVID-19 infected people are not in isolation, in which low-immune people such as older and other sick individuals can be affected by them [1]. Therefore, our goal is *to protect physical contact among the individuals* in an area such as a market, office, park, social community center, and others by recommending a risk-aware physical distance with a high-risk trajectory plan.

B. Related Work

The authors in [17] showed an analysis based on Bluetooth Low Energy signals of two smartphone users for mutual contact tracing. This analysis was considered for 15 minutes in a data-driven manner to detect optimal contact detection that was no more than 6 feet of distance. However, the authors did not consider when there are more than two people in a particular area. An evaluation of effectiveness on Bluetooth-based smartphone contact tracing application for COVID-19 performed by the author of [18]. Notably, the authors measured tracing speed for a centralized and decentralized approaches for newly possible infected individuals by COVID-19. However, this evaluation is conducted for a post-measurement that can control the future outbreak after affected but cannot prevent the infection of COVID-19. In [19], the authors proposed a social distancing monitoring system to prevent the spread of COVID-19 using oscillating magnetic field-based proximity sensing systems. The authors showed that for close-proximity (less than 2.0 m), the proposed oscillating magnetic field-based proximity sensing behaves more robust than Bluetooth. However, in the case of using this additional sensing system, individuals require to use an extra wearable device.

The authors in [20] proposed a sustainable lockdown policy for a government/organization based on the infection rate of COVID-19. In particular, the authors have captured tracking information of individuals using the Global Positioning System (GPS) through smart-phone. However, GPS can give approximate positioning for developing a sustainable lockdown policy, while in the case of real-time positioning of close-proximity the GPS does not work correctly. In [21], the authors proposed a fog computing framework for tracing contact to prevent COVID-19. Bluetooth of the smart-phone is considered as an end device signaling to measure the contact tracing. In [22], the authors proposed a deep learning-based social distance monitoring framework for a smart city. In particular, the authors used three state-of-the-art object detection models (i.e., Faster R-CNN, SSD, and YOLO) to detect individual from the videos. However, only detecting and monitoring do not have impacts on reducing infected people, where we need to take proactive action. In [23], the authors built a prototype to assist the smart city lockdown by detecting human faces for strictly maintaining restrictions on public movements. In particular, the authors proposed a three-layered edge computing architecture to reduce the latency of face detection for smart cities. The study in [23] does not consider any contract tracing scheme, nor do they consider any physical/social distancing mechanism.

C. Contributions

To address the above circumstances, in this work, we propose a risk-aware physical distancing recommender to reduce the risk of affected by the COVID-19 or such kind of pandemic due to inter-personal physical contact. This work is an extension of our initial findings in [24], and we summarize the significant contributions of this work as follows:

- First, we formulate a problem of risk-aware physical distancing for a Bluetooth-enabled personal area network. In particular, we capture a tail-risk by considering the Conditional-Value-at-Risk metric for a safe distance estimation of the PAN creator to enhance a private safety distance from others.
- Second, we propose a probabilistic linear model-based algorithm to solve the risk-aware physical distancing problem. Furthermore, this algorithm can effectively cope with the CVaR for estimating the safe distance among the individuals.
- Third, we have proposed the Levenberg-Marquardt-based curve-fitting scheme to recommend a high-risk trajectory plan of the PAN creator for ensuring private physical safety distance from others.

TABLE I
SUMMARY OF NOTATIONS

Notation	Description
c	PAN creator
$\mathcal{J}$	Set of users in PAN
p_c	Transmit power by PAN creator c to others $\mathcal{J}$
$R_{j\to c}$	RSSI received by c from user j
$d_{c\to j}$	Distance between PAN creator c and user j
Δ	Measured power of c
Θ	Environmental factor of the considered area
$z_{c\to j}(d_{c\to j})$	Zone label of user j
$v_{c\to j}$	Safe distance between user j and PAN creator c
α	Significance probability level
ζ	CVaR confidence
x	Safe-movement distance of a PAN creator c
$\mathcal{X}$	Set of safe-movement decision vectors $\boldsymbol{x}$
β, γ	Optimization parameters of the Levenberg-Marquardt-based curve fitting model
$\hat{\boldsymbol{x}}$	Vector of a high-risk zone trajectory

- Finally, experiment results show that the proposed solution approaches can efficiently determine safe movement distance for the PAN creator. And also capable of providing an optimal high-risk trajectory plan to ensure private safety from the COVID-19 or such kind of pandemic. Specifically, the proposed solution can deal with 45.11% of the CVaR for 95% CVaR-confidence.

The rest of the paper is organized as follows: we present the system model and problem formulation of the risk-aware physical distancing problem in Section II. In Section III, we represent the solution approach to the formulated problem. We discuss in detail experimental analysis in Section IV. Finally, we present our concluding remark in Section V.

II. System Model and Problem Formulation

A. System Model of Bluetooth-Based PAN

Considering an area that encompassed $J+1$ smart device users. In which one of the users c creates a personal area network (PAN) via the Bluetooth. Thus, the PAN creator c transmits wireless power p_c [dBm] to a set $\mathcal{J} = \{1, 2, \ldots, J\}$ of J smart device users in the considered coverage area (summary of notations is presented in Table I). Then each smart device $j \in \mathcal{J}$ sends back RSSI $R_{j\to c}$ from its current position to the PAN creator c. By capturing the RSSI $R_{j\to c}$ from each smart device $j \in \mathcal{J}$, the PAN creator c can determine its current distance from each user $j \in \mathcal{J}$. Thus, a distance $d_{c\to j}$ between PAN creator c and a smart device user j can be calculated as follows [3]:

$$d_{c\to j} = 10^{(\Delta - R_{j\to c})/(10\Theta)}, \tag{1}$$

where Δ represents measured power (i.e., $\Delta = -69$dBm [3]), and an environmental factor denotes by Θ. The value of Θ relies on the current environment of the PAN, where $\Theta = [2, 3, 4]$. This environmental factor directly affects with the correctness of a distance calculation between PAN creator c and each user $j \in \mathcal{J}$. We consider three zones [1] based on the current distance $d_{c\to j}$ between PAN creator c and each user $j \in \mathcal{J}$: 1) high-risk zone, 2) moderate risk zone, and 3) safe zone. In particular, each user $j \in \mathcal{J}$ belongs to one of these zones based on current distance $j \in \mathcal{J}$ [meter] (as seen in Figure 1). Therefore, the zone of each user $j \in \mathcal{J}$ is assigned as follows:

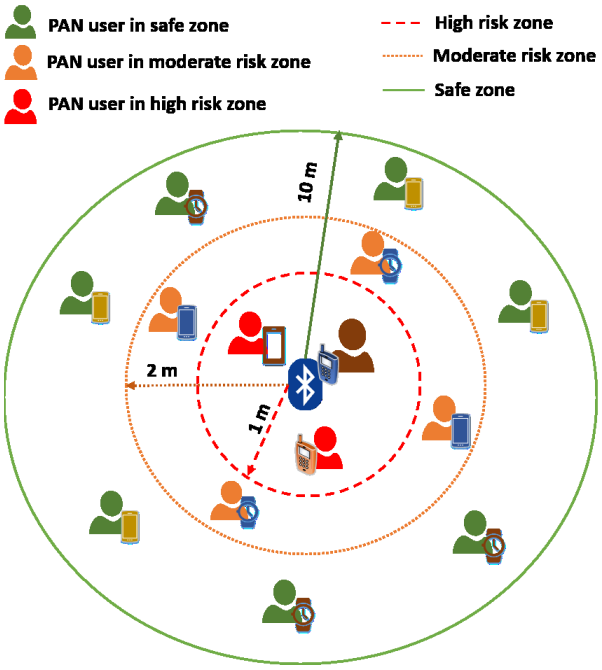

Fig. 1. System model of Bluetooth-based personal area network (PAN).

$$z_{c\to j}(d_{c\to j}) = \begin{cases} 0, & \text{if } d_{c\to j} \le 1, \\ 1, & \text{if } d_{c\to j} > 1 \ \& \ d_{c\to j} \le 2, \\ 2, & \text{otherwise}, \end{cases} \tag{2}$$

where 0, 1, and 2 represent a high risk, moderate risk, and safe zone, respectively. We consider an achievable safety distance $v_{c\to j}$ [meter] of PAN creator c from each user $j \in \mathcal{J}$. Thus, to reach a safety distance $v_{c\to j}$, the PAN creator c needs to move a certain amount of distance from its current position. Therefore, we consider x as a safe movement distance of the PAN creator c. This secure movement distance x is random over time and uncertain in nature. Therefore, we consider a safe movement distance decision vector $\boldsymbol{x} \in \mathbb{R}^J$, where $x \in \boldsymbol{x}$, and $\boldsymbol{x}$ is a random variable. Now we consider a function $\Lambda(\boldsymbol{x}, \boldsymbol{d})$ to determine a safe movement distance for the PAN creator c, where a decision of a safe movement distance x belongs to vector $\boldsymbol{x} \in \mathbb{R}^J$.

Additionally, we need to take into account the uncertain moves of the other PAN users $\forall j \in \mathcal{J}$ since they also can move inside the considered PAN. Therefore, we consider a set $\mathcal{X} = \{\boldsymbol{x}_1, \boldsymbol{x}_2, \ldots, \boldsymbol{x}_J\}$ of safe movement decision vectors $\boldsymbol{x} \subset \mathbb{R}^J$ for coping with the uncertainty of other users' movement over time. We denote a vector $\boldsymbol{d} \in \mathbb{R}^J$ to capture the randomness of all users, $\forall j \in \mathcal{J}$ with respect to each user's current distance $d_{c\to j}$ between the PAN creator c and each user $j \in \mathcal{J}$. Thus, we can determine a safe movement distance for the PAN creator as follows:

$$\Lambda(\boldsymbol{x}, \boldsymbol{d}) = \min_{\boldsymbol{x}\in\mathcal{X}} \mathbb{E}_{d_{c\to j}\sim P(\boldsymbol{d})}\Big[\sum_{j\in\mathcal{J}} |(x + d_{c\to j}) - v_{c\to j}|\Big], \tag{3}$$

where $P(\boldsymbol{d})$ is a probability distribution of current distances from PAN creator c to all users $\forall j \in \mathcal{J}$ for the considered PAN. Further, decision for a safe movement distance $x \in \boldsymbol{x} \in \mathbb{R}^J$ depends on $P(\boldsymbol{d})$. Therefore, (3) it-self is a random variable for each $\boldsymbol{x} \in \mathbb{R}^J$. Additionally, (3) is a function of the absolute difference between a safe distance constant $\upsilon_{c\to j}$ and a reachable safe distance $x + d_{c\to j}$ (i.e., movable distance x). Therefore, (3) holds the following properties:

- $|(x + d_{c\to j}) - \upsilon_{c\to j}| \geq 0$, (3) is always positive.
- $|(x + d_{c\to j}) - \upsilon_{c\to j}| = 0$, if and only if $(x + d_{c\to j}) = \upsilon_{c\to j}$.
- $|(x + d_{c\to j}) - \upsilon_{c\to j}| = |\upsilon_{c\to j} - (x + d_{c\to j})|$, (3) is symmetry.
- $|(x + d_{c\to j}) - b| \leq |(x + d_{c\to j}) - \upsilon_{c\to j}| + |\upsilon_{c\to j} - b|$, thus, (3) holds a triangle inequality.

Thus, an absolute deviation of a safe movable distance $x \in \boldsymbol{x}$ is the absolute difference between $x + d_{c\to j}$ and $\upsilon_{c\to j}$, which depends on a probability distribution of $P(\boldsymbol{d})$. To capture this deviation of a safe movable distance $x \in \boldsymbol{x}$, we need to cope with the uncertain characteristics of $\boldsymbol{d}$ for all users (i.e., $\forall j \in \mathcal{J}$) in the considered PAN. For characterizing the randomness of $d_{c\to j}$ where $j \in \mathcal{J}$, we consider a Conditional Value-at-Risk (CVaR) assessment. In particular, the CVaR can cope with an amount of tail risk for any kind of uncertain move for each user $j \in \mathcal{J}$ over a specific time frame t (i.e., each $t = 200$ ms).

B. Problem Formulation of a Risk-Aware Physical Distancing System

Considering a CVaR confidence level ζ for determining a risk-aware safe distance between the PAN creator c and other users $\forall j \in \mathcal{J}$. Thus, we denote a probability distribution $F(\boldsymbol{x}, \zeta)$ of the safe movable distance function $\Lambda(\boldsymbol{x}, \boldsymbol{d})$ (i.e., (3)). This probability distribution $F(\boldsymbol{x}, \zeta)$ can satisfy the considered CVaR confidence level ζ. In particular, ζ represents a cutoff point for determining a distribution $F(\boldsymbol{x}, \zeta)$ of $\Lambda(\boldsymbol{x}, \boldsymbol{d})$ to capture a tail-risk for safe movable distance x. In fact, CVaR confidence ζ shows inverse characteristics (i.e., inversely proportional) to the safe movement distance function $\Lambda(\boldsymbol{x}, \boldsymbol{d})$. Therefore, a cumulative distribution function (CDF) of ζ can be defined when a safe movement distance $x \in \boldsymbol{x}$ becomes fixed. The CDF for a function of ζ is denoted as follows [14]:

$$F(\boldsymbol{x}, \zeta) = \int_{\Lambda(\boldsymbol{x},\boldsymbol{d}) \leq \zeta} P(\boldsymbol{d}) d\boldsymbol{d}. \tag{4}$$

Therefore, $F(\boldsymbol{x}, \zeta)$ (i.e., (4)) is a nondecreasing and continuous function w.r.t. CVaR confidence ζ [14] Hence, we can discretize CVaR $\Gamma_\alpha(\boldsymbol{x})$ of random variable $\boldsymbol{x}$ by quantifying a risk that is the beyond Value-at-Risk (VaR) $\zeta_\alpha(\boldsymbol{x})$ [14], [25], [26], where $\alpha \in (0, 1)$ represents any significance probability level of VaR and CVaR. In particular, we capture an extreme risk of a safe movement distance $\Lambda(\boldsymbol{x}, \boldsymbol{d})$ for the PAN creator c by utilizing cumulative distribution $F(\boldsymbol{x}, \zeta)$ of ζ. Let us consider $\alpha \in (0, 1)$ as a significance probability level for both Value-at-Risk $\zeta_\alpha(\boldsymbol{x})$ and Conditional-Value-at-Risk $\Gamma_\alpha(\boldsymbol{x})$. Here, both of them rely on a random variable $\boldsymbol{x}$ to safe movement distance. Thus, by considering any significant probability level α, we can characterize VaR $\zeta_\alpha(\boldsymbol{x})$ as follows:

$$\zeta_\alpha(\boldsymbol{x}) = \min_{\zeta \in \mathbb{R}} F(\boldsymbol{x}, \zeta) \geq \alpha, \tag{5}$$

where (5) can estimate a value for ζ by satisfying $F(\boldsymbol{x}, \zeta) \geq \alpha$. Here, VaR $\zeta_\alpha(\boldsymbol{x})$ is an upper-bound that assists to capture a tail-risk for safe movement distance calculation. Therefore, we can capture CVaR $\Gamma_\alpha(\boldsymbol{x})$ for decision vector $\boldsymbol{x}$ (i.e., safe movement distance) of the PAN creator c as follows:

$$\Gamma_\alpha(\boldsymbol{x}) = \min_{\zeta \in \mathbb{R}} \frac{1}{(1-\alpha)} \int_{P(\Lambda(\boldsymbol{x},\boldsymbol{d})) \geq \zeta_\alpha(\boldsymbol{x})} \Lambda(\boldsymbol{x}, \boldsymbol{d}) P(\boldsymbol{d}) d\boldsymbol{d}. \tag{6}$$

(6) determines a conditional expectation for the random variable of safe movement distance $\boldsymbol{x}$, where $P(\Lambda(\boldsymbol{x}, \boldsymbol{d})) \geq \zeta_\alpha(\boldsymbol{x}) = (1-\alpha)$. To assure a private safety distance of the PAN creator c, individual needs to move at least x distance from its current position. Therefore, by characterizing the CVaR $\Gamma_\alpha(\boldsymbol{x})$, a risk-aware physical distancing problem can be defined as follows:

$$\Upsilon_\alpha(\boldsymbol{x}, \zeta) = \min_{\zeta \in \mathbb{R}} \zeta + \frac{1}{(1-\alpha)} \int_{\boldsymbol{d} \in \mathbb{R}^1} [F(\boldsymbol{x}, \zeta) - \zeta]^+ P(\boldsymbol{d}) d\boldsymbol{d}, \tag{7}$$

where $[F(\boldsymbol{x}, \zeta) - \zeta]^+$ is a function of ζ and positive. Additionally, $\Upsilon_\alpha(\boldsymbol{x}, \zeta)$ is a continuous function since (4) (i.e., $F(\boldsymbol{x}, \zeta)$) becomes continuous [14]. The goal of the problem (7) is to find safe movement distance $x \in \boldsymbol{x}$ of the PAN creator c while considering a distribution of ζ. In particular, the distribution of ζ satisfies $P(\Lambda(\boldsymbol{x}, \boldsymbol{d})) \geq \zeta_\alpha(\boldsymbol{x})$ to capture a tail of risk.

We propose a probabilistic linear model to solve the risk-aware physical distancing problem (7) by incorporating a probabilistic linear model. Next, based on the movable safety distance $\forall x_{c\to j} \in \boldsymbol{x}$ of the PAN creator c, we employ a curve-fitting [27] optimization to determine the recommended risk-zone of that individual. In particular, we decide a high-risk trajectory for c by solving a first degree polynomial equation to find an exact fit among the others $\forall j \in \mathcal{J}$ in the considered PAN. We describe our solution approaches in the following section.

III. Solution Approach of Risk-Aware Physical Distancing

In this section, we discuss the proposed solution approach to the risk-aware physical distancing system. Figure 2 illustrates an overall solution procedure of the risk-aware physical distancing problem. In particular, we propose two stages of solution procedure for the proposed risk-aware physical distancing system. First, we estimate current distance from PAN creator to other users and assigned each user $j \in \mathcal{J}$ into one of the zone among three (i.e., high risk, moderate risk, and safe zone) using a control flow scheme. Next, we solve (7) to determine safe movable distance by considering a tail-risk assessment of a probabilistic linear model. Based on the current and safe movable distance between the PAN creator and all users, a curve fitting scheme is proposed to determine a high-risk zone path planning for the PAN creator. In this solution approach, we propose Algorithm 1 and Algorithm 2 for

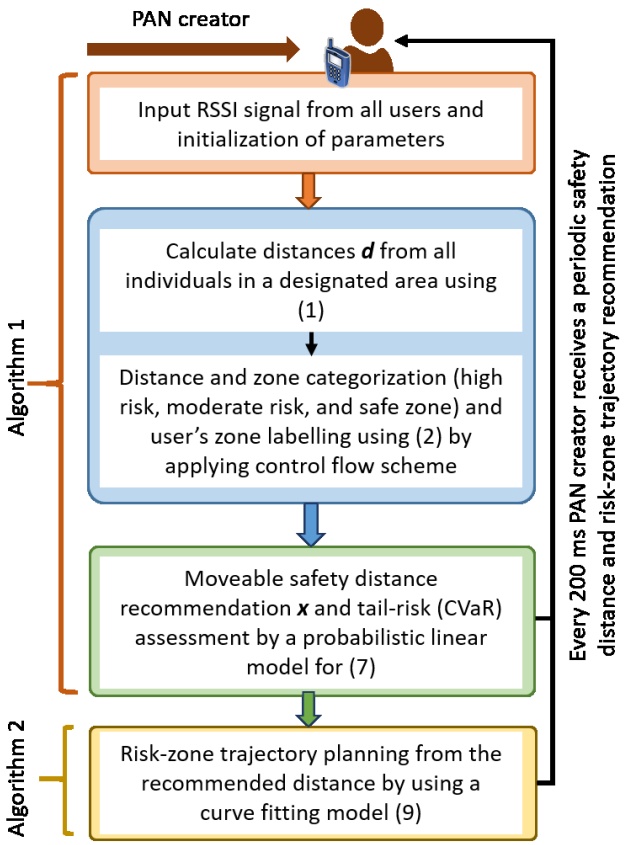

Fig. 2. Solution procedure of the proposed risk-aware physical distancing system.

Algorithm 1 Proposed Risk-Aware Physical Distancing Algorithm Based on Probabilistic Linear Model

Input: $R_{j\to c} \in \forall\mathcal{J}$, Δ, Θ, α
Output: $\boldsymbol{d}$, $\boldsymbol{x}$, $\hat{\boldsymbol{x}}$, $\forall\mathcal{J}$
Initialization: Δ, Θ, α, T, t, $z_{c\to j}(d_{c\to j}) \in \forall\mathcal{J}$, $\boldsymbol{d}, \forall\mathcal{J}$, ζ
1: **for Until:** $t \geq T$ **do**
2: **Broadcast:** p_c and **Receive:** $\forall R_{j\to c} \in \mathcal{J}$
3: **for** $\forall j \in \mathcal{J}$ **do**
4: **Distance:** $d_{c\to j} \in \mathcal{J}$ using (1)
5: **Zone:** $z_{c\to j}(d_{c\to j}) \in \mathcal{J}$ using (2)
6: **Append:** $d_{c\to j}$ to $\boldsymbol{d}$
7: **end for**
Risk-aware
8: safe movable distance and risk zone path planning
9: **for Until:** $P(\Lambda(\boldsymbol{x}, \boldsymbol{d})) \geq \zeta_\alpha(\boldsymbol{x})$ **do**
10: $sigma,\ mu = fit(\boldsymbol{d})$
11: $\zeta_\alpha(\boldsymbol{x}) = ppf(1-\alpha) * sigma - mu$ for (5)
12: $\Gamma_\alpha(\boldsymbol{x}) = \frac{1}{(1-\alpha)} * pdf(\zeta_\alpha(\boldsymbol{x})) * sigma - mu$ for (6)
13: **Estimate:** $\Upsilon_\alpha(\boldsymbol{x}, \zeta)$ for (7)
14: **end for**
15: **Send to Algorithm 2:** $(x_{c\to 1}, x_{c\to 2}, \ldots x_{c\to J}) \in \boldsymbol{x}$, $(d_{c\to 1}, d_{c\to 2}, \ldots d_{c\to J}) \in \boldsymbol{d}$, $\forall j \in \mathcal{J}$
16: **Receive:** risk-zone trajectory recommendation $\hat{x}_{c\to J}$ to $\hat{\boldsymbol{x}}$ of c from Algorithm 2
17: $t = t + 200$ ms
18: **end for**
19: **return**

Algorithm 2 Risk-Zone Trajectory Recommendation Based on Levenberg-Marquardt for PAN Creator c

Input: $(x_{c\to 1}, x_{c\to 2}, \ldots x_{c\to J}) \in \boldsymbol{x}$, $\forall j \in \mathcal{J}$, $(d_{c\to 1}, d_{c\to 2}, \ldots d_{c\to J}) \in \boldsymbol{d}$, $\forall j \in \mathcal{J}$
Output: $\hat{x}_{c\to j} \in \hat{\boldsymbol{x}}, \forall j \in \mathcal{J}$
Initialization: β, γ, $\boldsymbol{z}$
1: *fun_call*($\boldsymbol{d}$,β, γ)
2: *return* $\hat{x}_{c\to j} = f(d_{c\to j}, \boldsymbol{z}) = \beta\boldsymbol{d} + \gamma$
{Callback function for (8)}
3: β, γ = *optimize.curve_fit (fun_call,* $\boldsymbol{d}$, $\boldsymbol{x}$, $\boldsymbol{z}$)
{Using SciPy API [30] to execute (9) for finding β and γ}
4: **for Until:** $\forall j \in \mathcal{J}$ **do**
5: *fun_call*($\boldsymbol{d}$, β, γ) using (8)
6: **Append:** $\hat{x}_{c\to j}$ to $\hat{\boldsymbol{x}}$
7: **end for**
8: **Send:** risk-zone trajectory recommendation $\hat{\boldsymbol{x}}$ to Algorithm 1
9: **return**

determining risk-aware safe distance and risk zone trajectory planning of the PAN creator, respectively. Both Algorithms are deployed in a smart device of the PAN creator.

In Algorithm 1, PAN creator broadcasts power p_c to all users in PAN and receiving RSSI $\forall R_{j\to c} \in \mathcal{J}$ from these users in line 2. Line 4 estimates the current distance $d_{c\to j}$ between the PAN creator and each user $j \in \mathcal{J}$ in Algorithm 1 while line 5 assigns each user $j \in \mathcal{J}$ into a zone based on current distance. We solve (7) by developing a probabilistic linear model to find risk-aware movable safety distance for the PAN creator in lines 10 to 13 in Algorithm 1. In particular, line 10 of the Algorithm 1 estimates mean and variance using a distribution [28] of current users' distances $\boldsymbol{d}$. Algorithm 1 calculates the VaR (5) and CVaR (6) in lines 11 and 12, respectively. To determine safe movable distance decision $\boldsymbol{x}$ for the PAN creator c, the risk-aware physical distancing (7) problem is solved in line 13 of Algorithm 1.

Based on current distance $d_{c\to j} \in \boldsymbol{d}$ and risk-aware safety distance $x_{c\to j} \in \boldsymbol{x}$ between c and each user $j \in \mathcal{J}$, we estimate risk-zone trajectory using Algorithm 2. Thus, line 15 of Algorithm 1 sends $(x_{c\to 1}, x_{c\to 2}, \ldots x_{c\to J}) \in \boldsymbol{x}$ and $(d_{c\to 1}, d_{c\to 2}, \ldots d_{c\to J}) \in \boldsymbol{d}$ to Algorithm 2 while line 16 (in Algorithm 1) receives estimated risk-zone trajectory to recommend the PAN creator c. The above procedure is repeatedly executed for every $t = 200$ ms interval due to 200 ms is a desirable period for maintaining a stable PAN via Bluetooth. Thus, Algorithm 1 recommends to the PAN creator a safe distance among all users, and also providing a high-risk zone path planning using a Levenberg-Marquardt-based curve-fitting model (in Algorithm 2). Algorithm 1 can provide a solution to the PAN creator in polynomial time computational complexity while this complexity relies on the number of available users J in the PAN. Therefore, the computational complexity of the proposed Algorithm 1 leads to

$O(J^2)$ since Algorithm 1 can be reduced a base problem into a family of probabilistic linear model [28], [29].

We determine high-risk zone trajectory based on the available movable safety distance $\boldsymbol{x}$ for the PAN creator c from other users $\forall j \in \mathcal{J}$. To do this, we choose Levenberg-Marquardt (LM) algorithm [31] that is capable of faster convergence than Gauss-Newton (GN) [32] and Gradient Descent (GD) towards the optimizing its parameters for an optimal solution [33], [34]. Further, LM can select one direction from its possible two options, which ensures the robustness of the proposed solution approach. Additionally, the LM algorithm can still find an optimal solution although initial guess is far from the optima. LM has a trade-off for slow convergence when parameters contain a large vector [33], [34]. However, in this work, we consider a first degree polynomial equation with two parameters β and γ. Therefore, LM is a suitable choice to solve the following first degree polynomial equation,

$$\hat{x}_{c\to j} = f(d_{c\to j}, \beta, \gamma) = \beta \boldsymbol{d} + \gamma, \tag{8}$$

where $d_{c\to j} \in \boldsymbol{d}$ denotes current distance between PAN creator c and user $j \in \mathcal{J}$. We receive current distances $(d_{c\to 1}, d_{c\to 2}, \ldots d_{c\to J}) \in \boldsymbol{d}$ between PAN creator c and other users $\forall j \in \mathcal{J}$ from Algorithm 1. Subsequently, Algorithm 1 also provides safe movement distance $(x_{c\to 1}, x_{c\to 2}, \ldots x_{c\to J}) \in \boldsymbol{x}$ for the PAN creator c. In particular, $d_{c\to j} \in \boldsymbol{d}$ relies on $x_{c\to j} \in \boldsymbol{x}$ for determining a risk-zone trajectory between PAN creator c and each user j. Therefore, our goal is to determine parameters β and γ of (8), where the sum of the residual r is minimized,

$$r(\boldsymbol{x}, \boldsymbol{d}) = \min_{\beta,\gamma} \sum_{j=1}^{J} \left(x_{c\to j} - f(d_{c\to j}, \boldsymbol{z})\right)^2, \tag{9}$$

where $\boldsymbol{z} = (\beta, \gamma) \in \mathbb{R}^2$ denotes a vector of the parameters β and γ. We propose a Levenberg-Marquardt-based risk-zone trajectory planning Algorithm 2 for PAN creator c. In particular, we have applied the Levenberg-Marquardt algorithm through $scipy.optimize.curve\_fit$ API [30] for developing the proposed risk-zone trajectory Algorithm 2.

In Algorithm 2, inputs come from Algorithm 1 while we initialize parameters β and γ. We define a callback function in lines 1 and 2 of Algorithm 2 for solving (8). Then we utilize a standard solver for Levenberg-Marquardt algorithm using SciPy API [30] to execute (9) for finding β and γ. Line 3 of Algorithm 2 determines parameters β and γ for (9). In lines from 4 to 7, we estimate risk-zone trajectory for the PAN creator c to assure private safety from COVID-19 or such kind of pandemic. Finally, line 8 (in Algorithm 2) sends recommended risk-zone trajectory to the PAN creator c through Algorithm 1.

The Algorithm 2 solves a first degree polynomial equation based on Levenberg-Marquardt (LM) [31] method to recommend a high-risk trajectory plan for a personal area network (PAN) creator c. In particular, a nonlinear least squares problem (9) is solved by the Algorithm 2 in an iterative manner. Therefore, the number of iterations depends on an upper bound ϵ of $r(\boldsymbol{x}, \boldsymbol{d})$, such that $||\nabla r(\boldsymbol{x}, \boldsymbol{d})|| \leq \epsilon$ [35], [36].

TABLE II
SUMMARY OF EXPERIMENTAL SETUP

Description	Value
CVaR significance level α	$[0.90, 0.95, 0.99]$ [9]
Constant for RSSI effect on environmental Θ	$[2, 3, 4]$ [3]
Measured power of Bluetooth device Δ	-69 dBm [3]
No. of users in PAN J	$[1, 102953]$ [37]
Broadcast interval t	200 ms [37]
Observational duration T (minutes)	$[1, 3, 5, 10, 15, 30]$
Initial β	$[0.5, 1.0, 1.5, 2.0]$
Initial γ	$[0.5, 1.0, 1.5, 2.0]$
Probability distributions	Normal [28], Student-t [29]

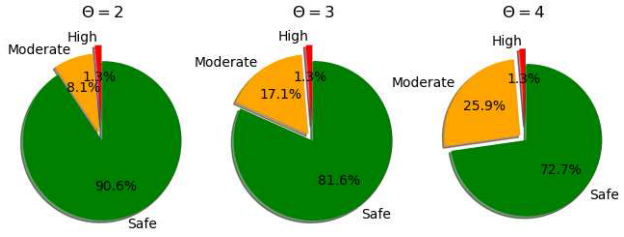

Fig. 3. Impact of environmental factor Θ for current distance estimation and zone categorization using RSSI.

As a result, the worst-case computational complexity of Algorithm 2 belongs to $O(J \times \epsilon^{-2})$, where J is the number of smart devices in the considered PAN. In fact, the worst-case computational complexity for a single phase of Algorithm 2 leads to $O(\epsilon^{-2})$ [35], [36]. Since the overall proposed solution of the risk-aware physical distancing problem based on a combined effort of Algorithms 1 and 2. In particular, Algorithm 2 receives input from Algorithm 1 to find an optimal high-risk trajectory plan for the PAN creator. While both Algorithms run on the same device (i.e., PAN creator's device). Therefore, in the proposed solution, there is no communication overhead regarding information sharing among the algorithms. Hence, the overall worst-case computational complexity of the risk-aware physical distancing problem becomes $O(J^2) + O(J \times \epsilon^{-2})$. In which, the complexity of Algorithm 1 solely depends on the number of smart devices J in the PAN, where $O(J^2)$ leads to a similar complexity of a probabilistic linear model [28], [29]. Further, the worst-case complexity $O(\epsilon^{-2})$ for a single-phase computation relies on an upper bound ϵ [35], [36] of Algorithm 2. Therefore, Algorithm 2 does not have any adverse effect on Algorithm 1 with respect to computational complexity, while the overall complexity leads to the family of polynomial-time $O(J^2)$.

To evaluate the effectiveness and reliability of proposed Algorithms 2 and 1 for solving the risk-aware physical distancing system, we have performed an extensive experimental analysis. We present in detail the experimental analysis and discussion in the following section.

IV. EXPERIMENTAL RESULTS AND DISCUSSION

In this experiment, we have considered RSSIReport dataset [37] to effectively measure the performance of the proposed Algorithm 1 and Algorithm 2. We have implemented these Algorithms on the python platform. Table II represents

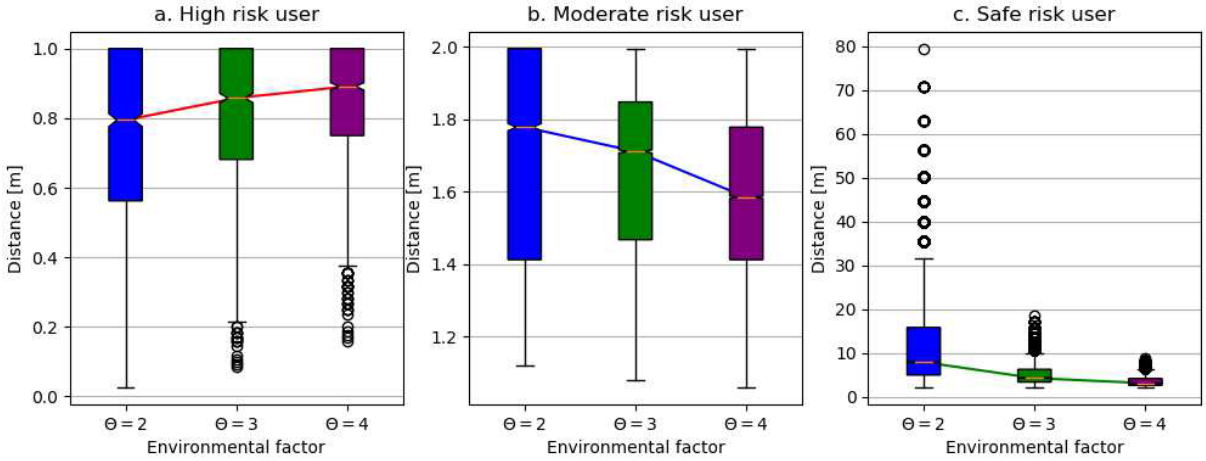

Fig. 4. An analysis of the impact of the environmental factor Θ for distance measurement through Bluetooth-based RSSI.

a summary of the experimental setup and other parameters considered the same as the dataset [37]. Further, we consider each beacon of the dataset [37] is a PAN creator. We have compared the normal distribution [28]-based linear model with a Student's t distribution [29]-based model in terms of CVaR risk assessment. Additionally, considered CVaR-based physical distancing model is compared with VaR for illustrating the strength of CVaR over the VaR. Finally, we have considered nearest-neighbor and cubic interpolation [38] as baselines to compare the proposed first degree polynomial for risk-zone trajectory planning. First, we illustrate an impact on distance measurement through Bluetooth-based RSSI over environmental factors $\Theta = [2, 3, 4]$ of a PAN creator in Figures 3 and 4. The Figure 3 shows that the number of high risk users (i.e., 1362 out of 102953) are the same for all values of $\Theta = [2, 3, 4]$. While in Figure 4 (a) shows that the median of distances vary for different Θ. In particular, the distance difference becomes around 100 cm for $\Theta = 2$ and $\Theta = 4$. Thus, we can conclude that $\Theta = 2$ is a suitable choice to ensure a robust distance measurement by the Bluetooth based RSSI in a very close proximity (i.e., 1 m^2). However, when the PAN coverage area increases, a higher Θ induces more users into the moderate risk zone from the safe zone as seen in Figure 3. Therefore, a higher value of Θ is a better choice for effectively measuring the distance via Bluetooth-based RSSI since it can capture the adversary effect from the environment for considered PAN. Therefore, a reliable safety distance measure is required before recommending a private safety distance of the PAN creator.

Second, an effectiveness analysis between a normal distribution and Student's t distribution [29] in terms of capturing tail-risk of CVaR for a distance estimation between PAN creator and others are shown in Figure 5. We have found that the self-movement distances of the PAN creator have 60.93% and 45.11% risk with respect to CVaR-confidences 99% and 95%, respectively within a range of 2 meters. Figure, 5 also illustrates that the Student's t distribution can significantly cope with the heavy tail process in terms of CVaR risk assessment. Therefore, we choose Student's t distribution-based model for further evaluation. As a result, the proposed method can

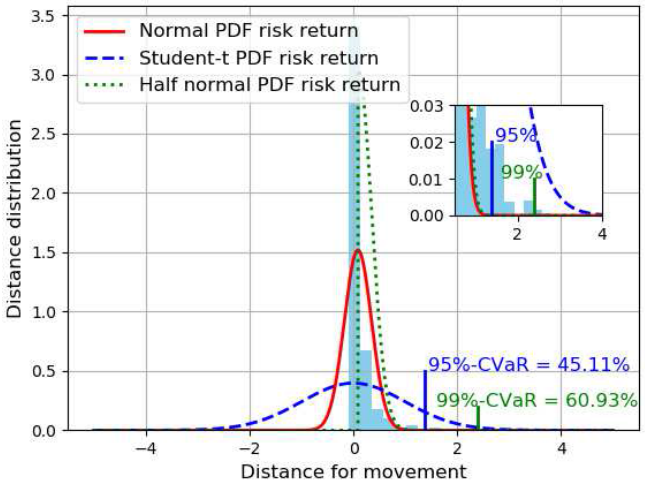

Fig. 5. Effectiveness analysis between a normal distribution and Student's t-distribution in terms of capturing tail-risk of CVaR for distance estimation.

effectively discretize a tail-risk from the Student's t distribution for measuring the distance in considered PAN. Thus, based on the outcomes of the proposed risk-aware physical distancing model, we can recommend a safe movable distance from all individuals to the PAN creator c.

Third, we analyze the performance of the proposed risk-aware physical distancing system in Figure 6 for 1, 3, 5, 10, 15, and 30 minutes of stay time to the PAN creator using Bluetooth beacon id 65 of the dataset [37]. Figure 6 shows that the risk between the considered individual and others is increasing from 0.2% to 6% when stay time goes from 1 minute to 30 minutes. In which, the proposed system can successfully detect those individuals into the risk-zone and capable of notifying to the system user.

Next, we illustrate the risk-zone trajectory planning for the user in Figure 7. In particular, the Figure 7 describes a high-risk path planning of the PAN creator c for 1, 3, and 5 minutes of stay duration in the considered PAN. We have found that the parameters (i.e., β and γ) value of the

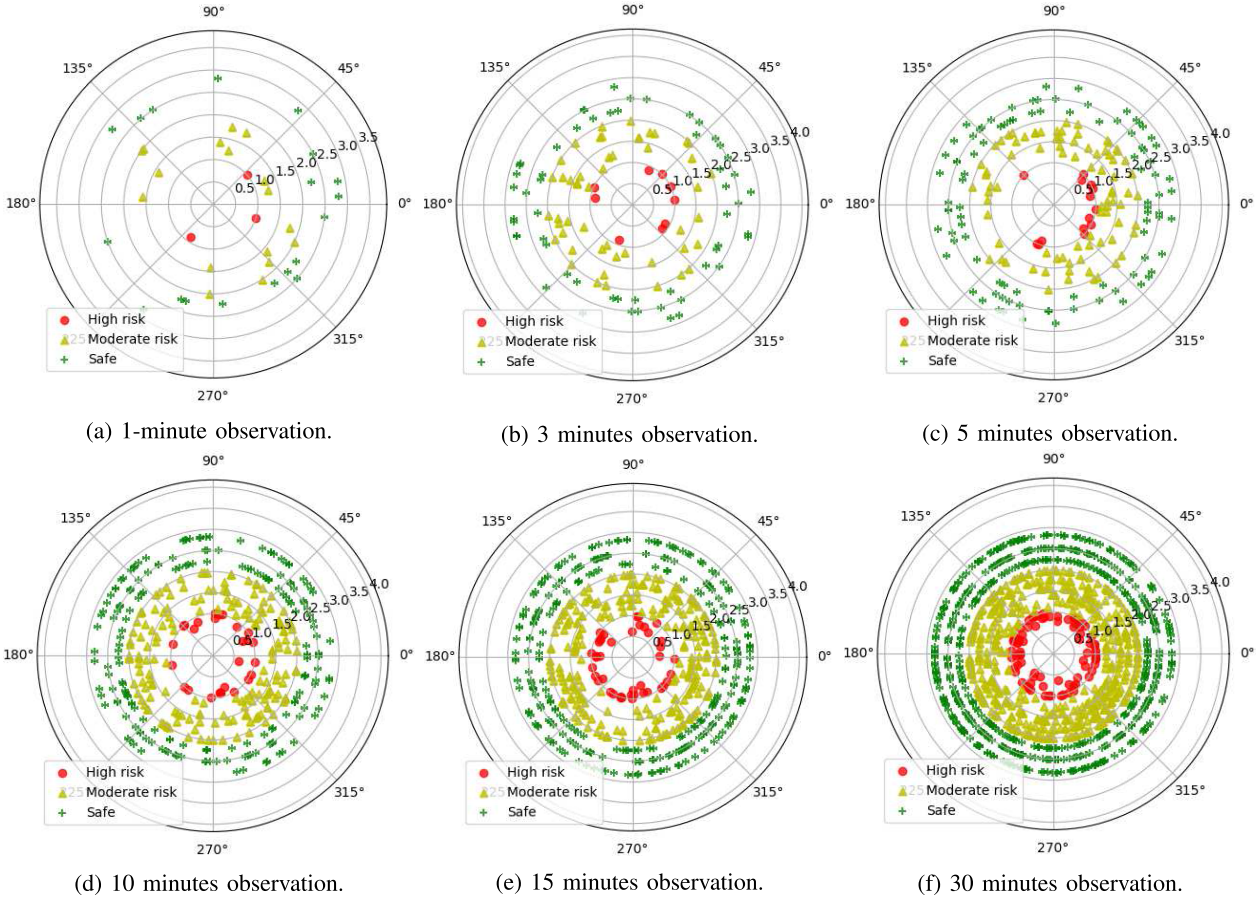

(a) 1-minute observation. (b) 3 minutes observation. (c) 5 minutes observation.

(d) 10 minutes observation. (e) 15 minutes observation. (f) 30 minutes observation.

Fig. 6. Private safety recommendation analysis for an individual during 1, 3, 5, 10, 15, and 30 minutes stay time with each 200 ms gap using the Bluetooth beacon id 80 of the dataset [37].

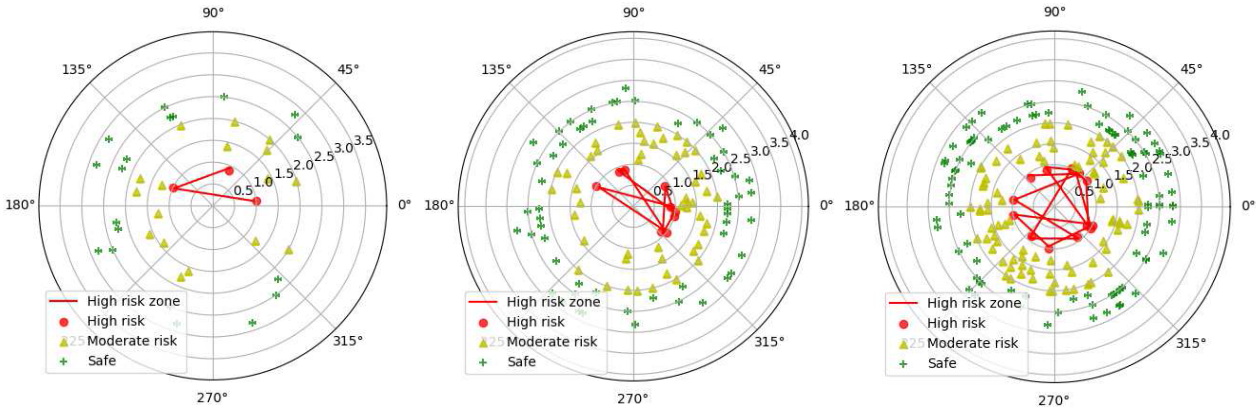

(a) 1-minute observation. (b) 3 minutes observation. (c) 5 minutes observation.

Fig. 7. High-risk path planning of an individual for 1, 3, and 5 minutes of stay duration with each 200 ms gap using the Bluetooth beacon id 80 of the dataset [37].

proposed Levenberg-Marquardt-based curve-fitting method, around $[0.0058668, 0.95598897]$, $[0.01097831, 0.8949547]$, and $[-0.00640721, 0.98195997]$ for 1, 3, and 5 minutes of stay duration, respectively. Thus, the proposed first-degree polynomial-based curve-fitting scheme can find an optimal path for risk-zone trajectory planning. Additionally, initialization of β and γ does not affect for obtaining the optimal parameters of the proposed Levenberg-Marquardt-based curve-fitting method (as seen in Table III) for the risk-zone path planning. In which, the LM algorithm can find an optimal solution while the initial guess is far from the optima [31], [33], [34]. In fact, we have implemented the LM algorithm through $scipy.optimize.curve\_fit$ API [30] for finding an optimal risk-zone path planning of the PAN creator. Thus, the proposed LM-based curve-fitting method of the risk-zone path planning scheme follows the nature of an optimal solution [31], [33], [34], while initialization of the parameters does not affect to obtain an optimal value.

TABLE III
INITIALIZATION VS. OPTIMAL PARAMETERS OF THE LEVENBERG-MARQUARDT-BASED CURVE-FITTING RISK-ZONE PATH PLANNING FOR A 5 MINUTES OBSERVATION IN PAN

Initial β	Initial γ	Optimal β^*	Optimal γ^*
0.5	0.5	-0.0005	0.9635
1.0	1.0	-0.0005	0.9635
1.5	1.5	-0.0005	0.9635
2.0	2.0	-0.0005	0.9635

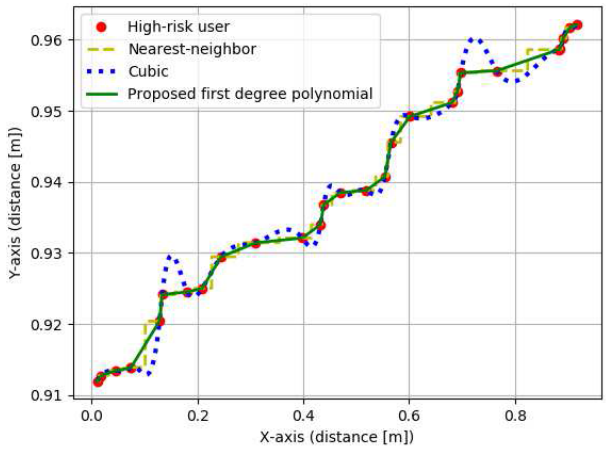

Fig. 8. A comparison of high-risk zone trajectory planning between the proposed and other baselines for 10 minutes observation.

In Figure 8, we have analyzed the effectiveness of a high-risk zone trajectory planning among the proposed first-degree polynomial and other baselines (i.e., nearest-neighbor and cubic). In this experiment, we have taken into account an area for the considered PAN. In which, we have experimented by considering a polar coordinate system. Thus, representing the interpolation difference between the proposed solution and baselines by a polar coordinate is not understandable. Therefore, we have illustrated Figure 8 into a two-dimensional plane instead of a polar axis. We have done this experiment by considering 10 minutes observation with a 200 ms intervals. The Figure 8 illustrates a high-risk zone trajectory planning for a 1 square meter area, where the interpolation of the proposed model significantly outperforms others by an exact fit over the high-risk users' current position.

Finally, a comparison between Value-at-Risk (VaR) and Conditional Value-at-Risk (CVaR) along with normal distribution and Student-t distribution for the recommended distance estimation is illustrated in Figure 9. For this analysis, we have considered beacon id 65 as a PAN creator where data are used from $2016-10-16:20:13:53$ to $2016-10-17:00:23:52$ of the dataset [37]. Thus, we have compared VaR and CVaR along with normal distribution and Student-t distribution in [37]. Figure 9 shows that the proposed CVaR-based model is more reliable than the VaR, in terms of tail-risk analysis when the environment is random over time. Therefore, the proposed model can significantly reduce the risk in terms of safety distance measurement and risk zone detection via Bluetooth in a PAN. To this end, this work not only analyses a theoretical perspective but also shown the practicality by implementing a smart-phone application on top of the Android platform [39] [See Appendix A]. In particular, we have collected RSSI signals from other smart devices via *BluetoothDevice device = intent.getParcelableExtra(BluetoothDevice.EXTRA_DEVICE)* [39]. Further, we have implemented the proposed risk-aware physical distancing application using open-source *Apache Commons* [40] APIs. Additionally, we have shared the implemented smart-phone application source code in a repository [1] to encourage an interested reader to reproduce or future usages. Therefore, the proposed risk-aware physical distancing system ensures theoretical robustness. Besides, we have validated the practicality by implementing a real-life smart device application.

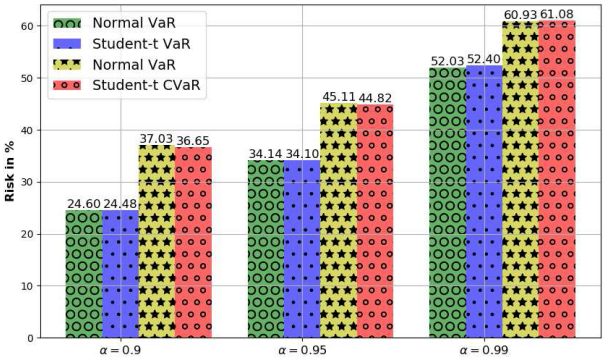

Fig. 9. A comparison between Value-at-Risk (VaR) and Conditional Value-at-Risk (CVaR) along with normal distribution and Student-t distribution for the distance estimation.

V. CONCLUSION

In this paper, we have introduced a novel risk-aware physical distancing problem for enhancing private safety that can help to resist the chance of affected by the COVID-19 or such kind of pandemic. We propose a Bluetooth-based PAN for effectively measuring a risk-aware physical distance between a PAN creator and nearby users using existing smart devices. In particular, we have proposed a CVaR-based physical distancing model and solved it by developing a probabilistic linear model that can efficiently cope with the tail-risk for distance estimation. Further, we have incorporated a curve-fitting optimization technique to find the optimal risk-zone trajectory so that the individual (i.e., PAN creator) can take proactive safety measures for reducing the risk of spreading COVID-19 or such kind of epidemic. Our experiment results show that the proposed approach can tackle about 45.11% of the risk for 95% confidence for physical distance calculation between the PAN creator and others. To this end, the newly-introduced risk-aware Bluetooth-PAN can significantly reduce the chance of spreading the COVID-19 by taking a proactive private safety measure.

APPENDIX A
RISK-AWARE PHYSICAL DISTANCING SYSTEM IMPLEMENTATION IN SMART DEVICE

We have implemented the proposed risk-aware physical distancing system on the Android platform [39] that ensures

[1] Android Application

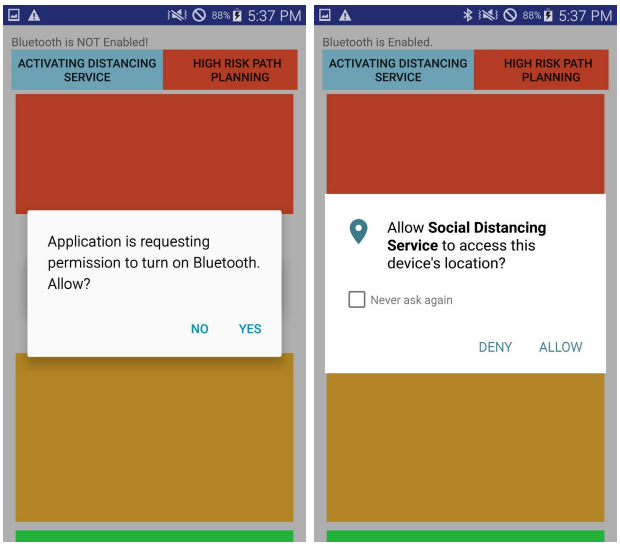

(a) Permission request for Bluetooth access. (b) Permission request for location access.

Fig. 10. Initial permission request for the social distancing service user in smart-device.

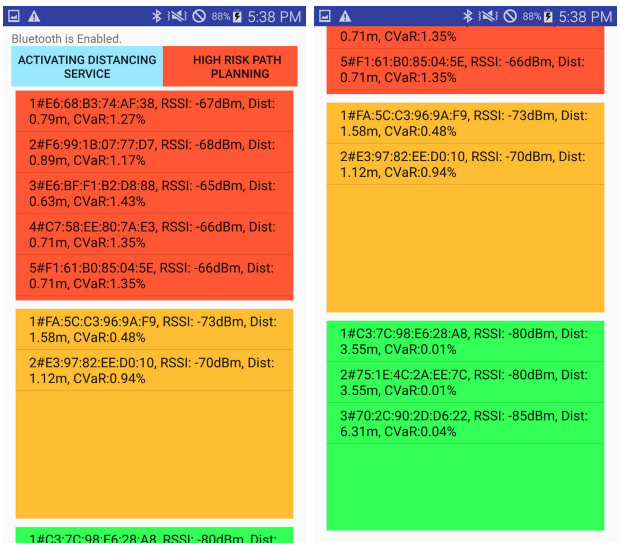

Fig. 11. Illustration of risk-zone categorization and RSSI, distance, and CVaR estimation between the social distancing service user and other users in an area.

(a) High-risk path planning at $4:46$ PM. (b) High-risk path planning at $4:47$ PM.

Fig. 12. High-risk path planning of the social distancing service user for a consecutive 2 minutes of duration.

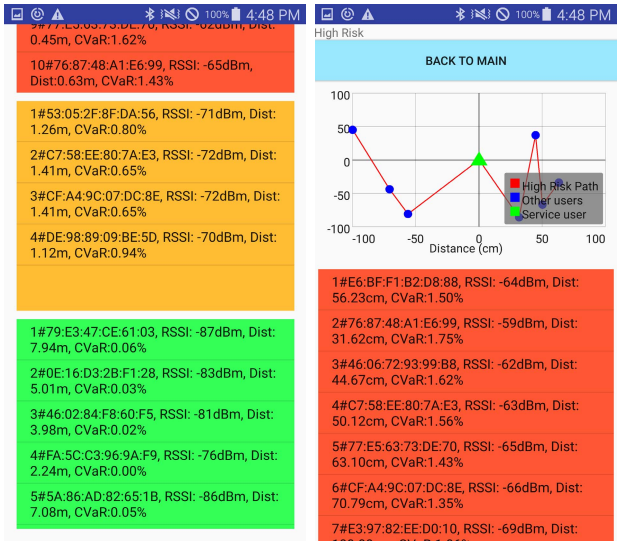

(a) All users in the range of the social distancing service user at $4:48$ PM. (b) High-risk path planning at $4:48$ PM for the social distancing service user.

Fig. 13. An example scenario of the proposed risk-aware physical distancing system in a smart-device application.

the practicality of the proposed system. However, the user interface design is out of the scope for this application development, where the main goal is to establish a proof of concept for the proposed system besides its theory.

Figure 10 represents the initial permission request for the social distancing service user in smart-device. We have demonstrated the risk-zone categorization and other outcomes (i.e., RSSI, distance, and CVaR between social distancing service user and other users) in Figure 11. In particular, in Figure 11, red, yellow, and green background colors in the developed application represent high-risk, moderate-risk, and safe users, respectively. Further, high-risk path planning for the social distancing service user for a consecutive 2 minutes of duration is illustrated in Figure 12. In order to demonstrate this, we consider a relative representation with respect to the current position of the social distancing service user in the considered area. In particular, we consider the social distancing service user (i.e., green color triangle) in the $(0, 0)$ position, while other users' (i.e., blue color circular shape) are surrounding based on the calculated distance (i.e., Algorithm 1) between the distancing service user and others. Further, we consider a range from -100 to 100 cm for both x-axis and y-axis to represent the high-risk area in the path planning graph of Figure 12. The high-risk path planning between the social dis-

tancing service user and other users represents with a red line curve in Figure 12 using the proposed Levenberg-Marquardt (LM)-based Algorithm 2. Finally, an example scenario of the proposed risk-aware physical distancing system of the developed smart-device application is demonstrated in Figure 13. In this experiment, we have considered 20 smart device users including the social distancing service user. In particular, Figure 13a shows risk-zone categorization (i.e., red, yellow, and green background colors) with respect to the social distancing service user. Further, we have illustrated a high-risk path planning for the social distancing service user's based on other high-risk users in the considered area in Figure 13b.

REFERENCES

[1] World Health Organization. (Mar. 19, 2020). *Considerations for Quarantine of Individuals in the Context of Containment for Coronavirus Disease (COVID-19): Interim Guidance*. Accessed: Oct. 12, 2020. [Online]. Available: https://apps.who.int/iris/handle/10665/331497

[2] K. Ueafuea *et al.*, "Potential applications of mobile and wearable devices for psychological support during the COVID-19 pandemic: A review," *IEEE Sensors J.*, vol. 21, no. 6, pp. 7162–7178, Mar. 2021.

[3] S. Sadowski and P. Spachos, "RSSI-based indoor localization with the Internet of Things," *IEEE Access*, vol. 6, pp. 30149–30161, 2018.

[4] S. M. Darroudi, C. Gomez, and J. Crowcroft, "Bluetooth low energy mesh networks: A standards perspective," *IEEE Commun. Mag.*, vol. 58, no. 4, pp. 95–101, Apr. 2020.

[5] B. Nagarajan, V. Shanmugam, V. Ananthanarayanan, and P. B. Bagavathi, "Localization and indoor navigation for visually impaired using Bluetooth low energy," in *Smart Systems and IoT: Innovations in Computing*. Singapore: Springer, Oct. 2019, pp. 249–259.

[6] P. H. O'Neill. (Apr. 22, 2020). *Bluetooth Contact Tracing Needs Bigger, Better Data*. MIT Technology Review. Accessed: Oct. 12, 2020. [Online]. Available: https://www.technologyreview.com/2020/04/22/1000353/bluetooth-contact-tracing-needs-bigger-better-data/

[7] F. Sainz. (Apr. 10, 2020). *Apple and Google Partner on COVID-19 Contact Tracing Technology*. Newsroom. Accessed: Oct. 12, 2020. [Online]. Available: https://www.apple.com/newsroom/2020/04/apple-and-google-partner-on-covid-19-contact-tracing-technology/

[8] M. S. Munir, S. F. Abedin, M. G. R. Alam, N. H. Tran, and C. S. Hong, "Intelligent service fulfillment for software defined networks in smart city," in *Proc. Int. Conf. Inf. Netw. (ICOIN)*, Chiang Mai, Thailand, Jan. 2018, pp. 516–521.

[9] M. S. Munir, S. F. Abedin, D. H. Kim, N. H. Tran, Z. Han, and C. S. Hong, "A multi-agent system toward the green edge computing with microgrid," in *Proc. IEEE Global Commun. Conf. (GLOBECOM)*, Waikoloa, HI, USA, Dec. 2019, pp. 1–7.

[10] M. S. Munir, S. F. Abedin, N. H. Tran, Z. Han, E.-N. Huh, and C. S. Hong, "Risk-aware energy scheduling for edge computing with microgrid: A multi-agent deep reinforcement learning approach," *IEEE Trans. Netw. Service Manage.*, early access, Jan. 5, 2021, doi: 10.1109/TNSM.2021.3049381.

[11] M. S. Munir, S. F. Abedin, and C. S. Hong, "Artificial intelligence-based service aggregation for mobile-agent in edge computing," in *Proc. 20th Asia–Pacific Netw. Oper. Manage. Symp. (APNOMS)*, Matsue, Japan, Sep. 2019, pp. 1–6.

[12] J. Haartsen, M. Naghshineh, J. Inouye, O. J. Joeressen, and W. Allen, "Bluetooth: Vision, goals, and architecture," *ACM SIGMOBILE Mobile Comput. Commun. Rev.*, vol. 2, no. 4, pp. 38–45, 1998.

[13] K. Michael and R. Abbas, "Behind COVID-19 contact trace apps: The Google–Apple partnership," *IEEE Consum. Electron. Mag.*, vol. 9, no. 5, pp. 71–76, Sep. 2020.

[14] R. T. Rockafellar and S. Uryasev, "Conditional value-at-risk for general loss distributions," *J. Banking Finance*, vol. 26, no. 7, pp. 1443–1471, Jul. 2002.

[15] Coronavirus Disease-19, Republic of Korea. *Social Distancing Continue*. Accessed: Feb. 2, 2021. [Online]. Available: http://ncov.mohw.go.kr/en

[16] World Health Organization. *I Am Vaccinated, What Next?*. Accessed: Feb. 2, 2021. [Online]. Available: https://www.who.int/emergencies/diseases/novel-coronavirus-2019/media-resources/science-in-5/episode-23—i-am-vaccinated-what-next?gclid=CjwKCAiAjp6BBhAIEiwAkO9WunMBAN9OSdryYvOTx1sOEV10zCe9Zepx_eTe-nxVI27iA8V39LAXxxoC2VcQAvD_BwE

[17] G. F. Hatke *et al.*, "Using Bluetooth low energy (BLE) signal strength estimation to facilitate contact tracing for COVID-19," 2020, *arXiv:2006.15711*. [Online]. Available: http://arxiv.org/abs/2006.15711

[18] E. Hernández-Orallo, C. T. Calafate, J. Cano, and P. Manzoni, "Evaluating the effectiveness of COVID-19 Bluetooth-Based smartphone contact tracing applications," *Appl. Sci.*, vol. 10, no. 20, p. 7113, Oct. 2020.

[19] S. Bian, B. Zhou, H. Bello, and P. Lukowicz, "A wearable magnetic field based proximity sensing system for monitoring COVID-19 social distancing," in *Proc. Int. Symp. Wearable Comput.*, Sep. 2020, pp. 22–26.

[20] A. K. Bairagi *et al.*, "Controlling the outbreak of COVID-19: A noncooperative game perspective," *IEEE Access*, vol. 8, pp. 215570–215581, Nov. 2020.

[21] M. Whaiduzzaman *et al.*, "A privacy-preserving mobile and fog computing framework to trace and prevent COVID-19 community transmission," *IEEE J. Biomed. Health Informat.*, vol. 24, no. 12, pp. 3564–3575, Dec. 2020.

[22] M. Shorfuzzaman, M. S. Hossain, and M. F. Alhamid, "Towards the sustainable development of smart cities through mass video surveillance: A response to the COVID-19 pandemic," *Sustain. Cities Soc.*, vol. 64, Jan. 2021, Art. no. 102582.

[23] M. Kolhar, F. Al-Turjman, A. Alameen, and M. M. Abualhaj, "A three layered decentralized IoT biometric architecture for city lockdown during COVID-19 outbreak," *IEEE Access*, vol. 8, pp. 163608–163617, Sep. 2020.

[24] M. S. Munir, D. H. Kim, S. F. Abedin, and C. S. Hong, "A risk-sensitive social distance recommendation system via Bluetooth towards the COVID-19 private safety," in *Proc. Korean Comput. Congr. (KCC)*, Jul. 2020, pp. 1028–1030.

[25] Y. Chow and M. Ghavamzadeh, "Algorithms for CVaR optimization in MDPs," in *Proc. 27th Int. Conf. Neural Inf. Process. Syst. (NIPS)*, vol. 2. Montreal, QC, Canada, Dec. 2014, pp. 3509–3517.

[26] P. Krokhmal, T. Uryasev, and J. Palmquist, "Portfolio optimization with conditional value-at-risk objective and constraints," *J. Risk*, vol. 4, no. 2, pp. 43–68, Mar. 2001.

[27] E. C. Levy, "Complex-curve fitting," *IRE Trans. Autom. Control*, vol. AC-4, no. 1, pp. 37–43, 1959.

[28] D. Clayton and M. Hills, *Statistical Models in Epidemiology*. Oxford, U.K.: Oxford Univ. Press, 2013, ch. 8.

[29] M. Roth, E. Ozkan, and F. Gustafsson, "A student's T filter for heavy tailed process and measurement noise," in *Proc. IEEE Int. Conf. Acoust., Speech Signal Process.*, Vancouver, BC, Canada, May 2013, pp. 5770–5774.

[30] Scipy. *Scipy.Optimize.Curve_Fit*. SciPy.org. Accessed: Oct. 12, 2020. [Online]. Available: https://https://docs.scipy.org/doc/scipy/reference/generated/scipy.optimize.curve_fit.html

[31] K. Levenberg, "A method for the solution of certain non-linear problems in least squares," *Quart. Appl. Math.*, vol. 2, no. 2, pp. 164–168, 1944.

[32] H. O. Hartley, "The modified Gauss-Newton method for the fitting of non-linear regression functions by least squares," *Technometrics*, vol. 3, no. 2, pp. 269–280, May 1961.

[33] J. J. Moré, "The Levenberg–Marquardt algorithm: Implementation and theory," in *Numerical Analysis*. Basel, Switzerland: Springer, 1978, pp. 105–116.

[34] D. W. Marquardt, "An algorithm for least-squares estimation of nonlinear parameters," *J. Soc. Ind. Appl. Math.*, vol. 11, no. 2, pp. 431–441, Jun. 1963.

[35] K. Ueda and N. Yamashita, "On a global complexity bound of the Levenberg–Marquardt method," *J. Optim. Theory Appl.*, vol. 147, no. 3, pp. 443–453, Dec. 2010.

[36] E. H. Bergou, Y. Diouane, and V. Kungurtsev, "Convergence and complexity analysis of a Levenberg–Marquardt algorithm for inverse problems," *J. Optim. Theory Appl.*, vol. 185, pp. 927–944, May 2020.

[37] D. Sikeridis, I. Papapanagiotou, and M. Devetsikiotis. (Mar. 2019). *CRAWDAD Dataset Unm/Blebeacon (V. 2019-03-12)*. traceset: RSSIReport. Accessed: Apr. 25, 2020. [Online]. Available: https://crawdad.org/unm/blebeacon/20190312/RSSIReport

[38] P. J. Davis, *Interpolation and Approximation*. Chelmsford, MA, USA: Courier Corporation, 1975.

[39] Android Developers Docs Guides. *Bluetooth Overview*. Accessed: Apr. 25, 2020. [Online]. Available: https://developer.android.com/guide/topics/connectivity/bluetooth

[40] Apache Commons. *Commons Math: The Apache Commons Mathematics Library*. Accessed: Feb. 2, 2021. https://commons.apache.org/proper/commons-math/

Md. Shirajum Munir (Graduate Student Member, IEEE) received the B.S. degree in computer science and engineering from Khulna University, Khulna, Bangladesh, in 2010. He is currently pursuing the Ph.D. degree in computer science and engineering with Kyung Hee University, Seoul, South Korea. He served as a Lead Engineer with the Solution Laboratory, Samsung Research and Development Institute, Dhaka, Bangladesh, from 2010 to 2016. His current research interests include the IoT network management, fog computing, mobile edge computing, software-defined networking, smart grid, and machine learning.

Do Hyeon Kim received the B.S. degree in communication engineering from Jeju National University in 2014, and the M.S. degree from Kyung Hee University in 2017, where he is currently pursuing the Ph.D. degree with the Department of Computer Science and Engineering. His research interests include multiaccess edge computing and wireless network virtualization.

Anupam Kumar Bairagi (Member, IEEE) received the B.Sc. and M.Sc. degrees in computer science and engineering from Khulna University (KU), Bangladesh, and the Ph.D. degree in computer engineering from Kyung Hee University, South Korea. He is an Associate Professor with the Computer Science and Engineering Discipline, Khulna University. He has authored and coauthored around 40 publications, including refereed IEEE/ACM journals and conference papers. His research interests include wireless resource management in 5G and beyond, healthcare, the IIoT, cooperative communication, and game theory. He has served as a technical program committee member for different international conferences.

Choong Seon Hong (Senior Member, IEEE) received the B.S. and M.S. degrees in electronic engineering from Kyung Hee University, Seoul, South Korea, in 1983 and 1985, respectively, and the Ph.D. degree from Keio University, Tokyo, Japan, in 1997. In 1988, he joined KT, Gyeonggi, South Korea, where he was involved in broadband networks as a member of the Technical Staff. Since 1993, he has been with Keio University. He was with the Telecommunications Network Laboratory, KT, as a Senior Member of Technical Staff and as the Director of the Networking Research Team until 1999. Since 1999, he has been a Professor with the Department of Computer Science and Engineering, Kyung Hee University. His research interests include future Internet, intelligent edge computing, network management, and network security. Dr. Hong is a member of the Association for Computing Machinery (ACM), the Institute of Electronics, Information and Communication Engineers (IEICE), the Information Processing Society of Japan (IPSJ), the Korean Institute of Information Scientists and Engineers (KIISE), the Korean Institute of Communications and Information Sciences (KICS), the Korean Information Processing Society (KIPS), and the Open Standards and ICT Association (OSIA). He has served as the General Chair, the TPC Chair/Member, or an Organizing Committee Member of international conferences, such as the Network Operations and Management Symposium (NOMS), the International Symposium on Integrated Network Management (IM), the Asia-Pacific Network Operations and Management Symposium (APNOMS), the End-to-End Monitoring Techniques and Services (E2EMON), the IEEE Consumer Communications and Networking Conference (CCNC), the Assurance in Distributed Systems and Networks (ADSN), the International Conference on Parallel Processing (ICPP), the Data Integration and Mining (DIM), the World Conference on Information Security Applications (WISA), the Broadband Convergence Network (BcN), the Telecommunication Information Networking Architecture (TINA), the International Symposium on Applications and the Internet (SAINT), and the International Conference on Information Networking (ICOIN). He was an Associate Editor of the IEEE TRANSACTIONS ON NETWORK AND SERVICE MANAGEMENT and the IEEE JOURNAL OF COMMUNICATIONS AND NETWORKS and an Associate Editor of the *International Journal of Network Management* and an Associate Technical Editor of the *IEEE Communications Magazine*. He currently serves as an Associate Editor for the *International Journal of Network Management* and *Future Internet* Journal.